Structural characterization of cadmium selenide thin films by X-ray diffraction and electron microscopy

1992 J. Phys. D: Appl. Phys. 25 1488

(http://iopscience.iop.org/0022-3727/25/10/014)

J. Phys. D: Appl. Phys. 25 (1992) 1488–1494. Printed in the UK

Structural characterization of cadmium selenide thin films by x-ray diffraction and electron microscopy

U Pal†, D Samanta‡, S Ghorai‡, B K Samantaray† and A K Chaudhuri†

† Department of Physics and Meteorology, Indian Institute of Technology, Kharagpur-721 302, India
‡ Department of Physics, Vidyasagar University, Midnapore-721 101, India

Received 20 September 1991, in final form 22 April 1992

Abstract. X-ray diffraction, transmission electron microscopy and transmission electron diffraction studies on cadmium selenide thin films deposited on glass substrates have been carried out. X-ray line profile analysis of the diffraction patterns has been performed to study the microstructural parameters. The variation of different microstructural parameters, such as crystallite size, RMS strain, dislocation density and stacking fault probability with film thickness as well as substrate temperature is studied. The optimum growth condition is fixed to a film thickness of the order of 1.0 μm. The change of preferred orientation is observed for films deposited at and above 473 K.

1. Introduction

Among the II–VI compounds, cadmium selenide is an important material for the fabrication of hetero-junction solar cells and photo-electrochemical solar cells. Due to its suitable direct band gap (1.70 eV) and high photosensitivity in the visible range of the solar spectrum, a large number of workers (Heller *et al* 1977, Miller and Hanemann 1981, Boudrau and Rauh 1982) have studied the growth condition of thin films for use in device fabrication. The crystallite structure of CdSe has been studied by Samarath *et al* (1990)—they studied the crystalline structure of CdSe in wurtzite form. Ueno *et al* (1987) studied the growth condition of CdSe thin films on glass substrates deposited by chemical methods and showed the composition and particle size variation with different growth conditions by x-ray and electron microscopy. Givargizov (1974) has described the growth of needle and plate crystals of CdSe from vapour on single crystal CdSe substrate with {001} orientation. Many workers (Thutupalli and Tomlin 1976, El-Shazly *et al* 1986) have grown CdSe thin films on glass and quartz substrates. Epitaxial growth of CdSe films on single crystal wafer sapphire {001} substrates was described by Yim and Stofko (1974) and Ratcheva-Stambolieva *et al* (1973) by vacuum evaporation and CVD techniques respectively. The structure of CdSe films created by tarnishing on Cd rod/plates and titanium films was studied by Curran *et al* (1986) by x-ray and electron microscopy.

Though a quantitative estimation of particle size and its variation with substrate temperature and deposition rate was made by Naguib *et al* (1979) for thin films of CdSe deposited on Corning 7089 substrates, a detailed quantitative study of different microstructural parameters and their dependence on the growth conditions for CdSe films on glass substrates has not been presented to date. In the present study determination of different microstuctural parameters such as favourable orientation, particle size, RMS strain, stacking fault probability etc, is reported for CdSe thin films by x-ray line profile analysis, TEM and TED techniques. The effects of film thickness, substrate temperature and stoichiometry on these microstructural parameters have been studied.

2. Experiment

Cadmium selenide was synthesised in a quartz ampoule taking cadmium (99.999%) and selenium (99.999%) in their own atomic weight ratio. The ampoule was evacuated to $\sim 10^{-4}$ Pa and sealed. The synthesis of the material was done in a vertical tantalum furnace. The ampoule was kept at the uniform temperature zone of the furnace. The temperature of the furnace was raised from 473 K to 1173 K slowly and kept at this temperature for about twelve hours. The temperature was then raised to 1523 K quickly to avoid constitutional supercooling. The ampoule was kept at this tem-

0022-3727/92/101488 + 07 $04.50

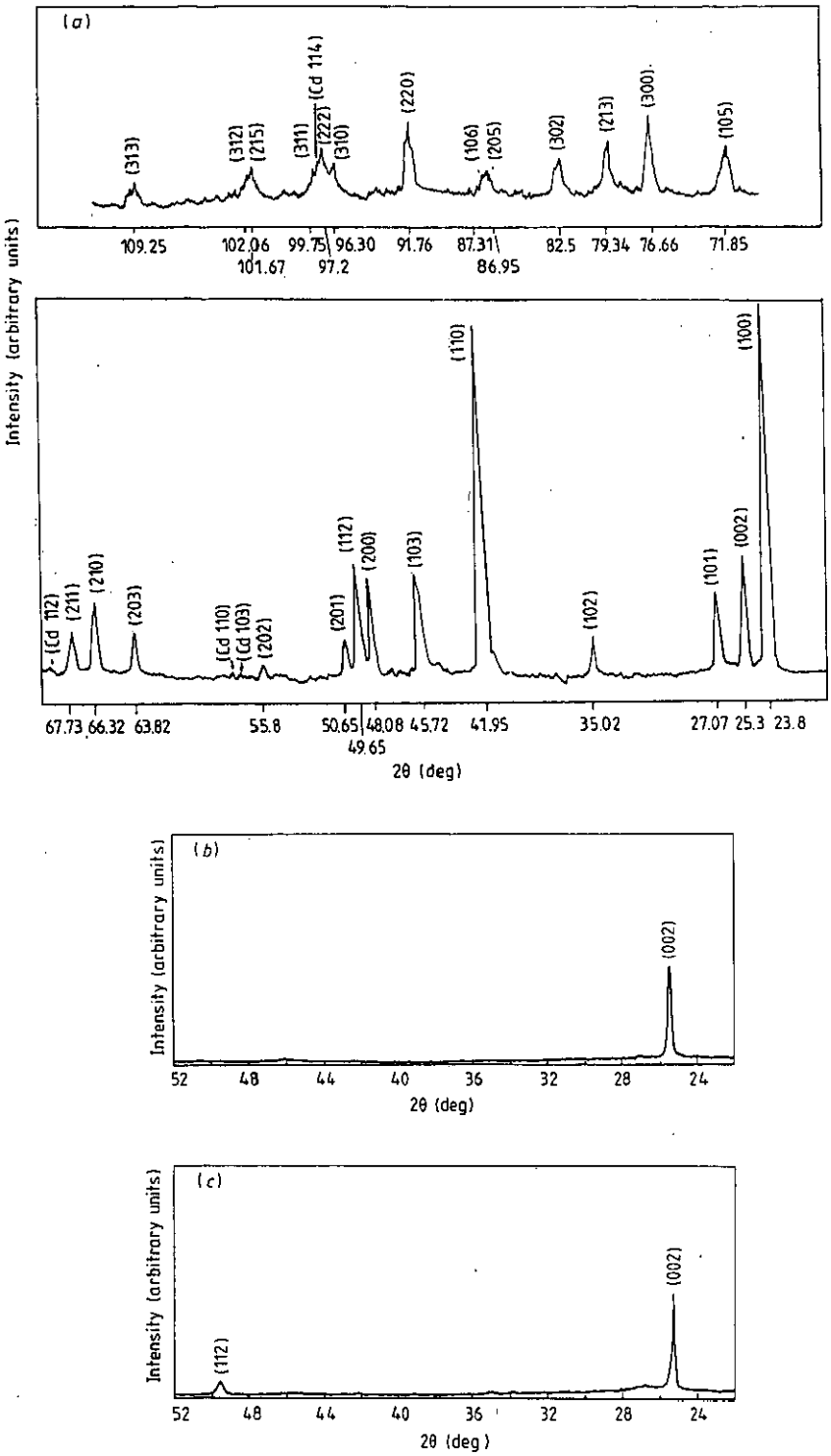

Figure 1. X-ray diffraction pattern of (*a*) CdSe powders (*b*) a CdSe thin film of 280 nm thickness deposited at room temperature and (*c*) a CdSe thin film of 290 nm thickness deposited at 623 K substrate temperature using CuK_{α} radiation.

perature for 30 min. The furnace was then cooled to 873 K and the ampoule was removed and quenched in air. The material did not adhere to the quartz wall. At a temperature above 1173 K the reverse reaction (CdSe → Cd + Se) starts; for this reason the ampoule was kept at this temperature for sufficient time to complete the reaction. Even then, an unreacted portion of the elements may be left for constitutional supercooling, and lack of knowledge exists about the exact completion of the reaction. It was therefore necessary to increase the temperature of the furnace well above the melting point of the compound. X-ray powder diffraction of the synthesised material confirmed the formation of cadmium selenide compound with some excess of cadmium. Figure 1(*a*) shows the x-ray powder diffraction pattern of the grown sample.

The films of cadmium selenide were deposited by evaporating CdSe powders from a molybdenum boat in vacuum of the order of 10^{-4} Pa on properly cleaned glass substrates. Deposition was made with the help of a Hind Hivac coating unit (model 12-A4). The rate of deposition was maintained at 120 nm min^{-1} for the films deposited at room temperature. However, for the films deposited at different substrate temperatures, the rate of deposition was kept at 150 nm min^{-1}. The deposition of the films at high temperatures were carried out in suitable apparatus described elsewhere (Santhanam *et al* 1982). The thickness of the films was measured by a Taylor–Hobson Form talysurf. The x-ray diffractograms are recorded with the help of a Phillips x-ray diffractometer (PW 1729) at a scanning speed of 0.5° min^{-1} using CuK_α radiation. Transmission electron micrographs (TEM) and transmission electron diffraction (TED) patterns were obtained with the help of an electron microscope (JEOL, JEM 200CX). The composition of the films was estimated by EDAX using a Camscan series II DV electron microscope with link system.

The diffracted x-ray intensities from the films were of polycrystalline type and the line profiles were subjected to variance analysis (Mitra 1964) to calculate the crystallite size and microstrain values. Since the method is sensitive to variation near the tails of the peaks, a careful adjustment of the background was carried out following the method of Mitra and Misra (1966). Since the variances are additive, the profiles were corrected for instrumental broadening by subtracting the variance of the corresponding profile for standard well annealed CdSe samples. If it is assumed that the broadening of the x-ray line is due to crystallite size and strain only, the variance can be written as

$$W_{2\theta} = \lambda\sigma/(2\pi^2 p\cos\theta) + 4\tan^2\theta\langle e^2\rangle \qquad (1)$$

where σ is the angular range, p the crystallite size, $\langle e^2\rangle$ is the mean squared strain, λ the wavelength of x-ray and θ the Bragg angle.

Dislocation density, as defined by Hirsch (1956), is the length of dislocation line per unit volume of the crystal. Williamson and Smallman (1956) suggested two methods for calculating the dislocation densities; one is from particle size values and the other from the strain. Since both the particle size and RMS strain are manifestations of dislocation network in the films, the dislocation density given by Williamson and Smallman (1956) can be expressed as

$$\rho = (3nK/F)^{1/2}\langle e^2\rangle^{1/2}/(bp) \qquad (2)$$

where p is the particle size, $\langle e^2\rangle^{1/2}$ the RMS strain, b the Burgers vector, n the number of dislocations on each face of the particle, K the constant depending on the strain distribution and F is an interaction parameter. For Cauchy strain profiles the value of K is about 25, whereas for Gaussian strain profiles it is nearly four. In the absence of extensive polygonization, dislocation density can be calculated from equation (2) assuming $n \simeq F$, $b = d$ (the interplanar spacing) and $K = 4$. Now

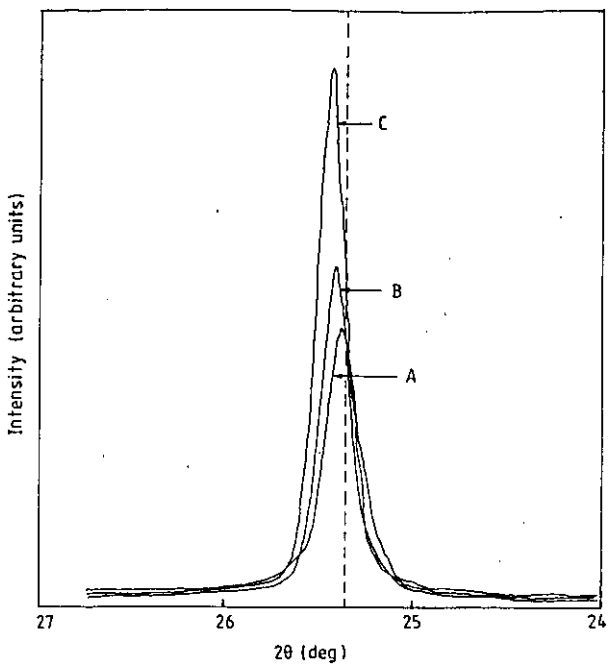

Figure 2. X-ray diffraction profile of A, 342 nm; B, 673 nm; and C, 1007 nm CdSe films showing the peak shift and line broadening. The broken line shows the peak position of the well annealed powdered sample.

equation (2) reduces to

$$\rho = \sqrt{12}\langle e^2\rangle^{1/2}/(dp). \qquad (3)$$

Hexagonal wurtzite crystals are formed by stacking of the densely packed {001} planes in proper sequence AB AB AB . . .. A deviation in sequence gives rise to a fault in it. In the hexagonal wurtzite crystals of 2H type, the fault in the stacking sequence occurs like AB AB CA CA CA.

The stacking fault probability α is the fraction of layers undergoing stacking sequence faults in a given crystal, and hence one fault is expected to be found in $1/\alpha$ layers. Occurrence of stacking faults gives rise to

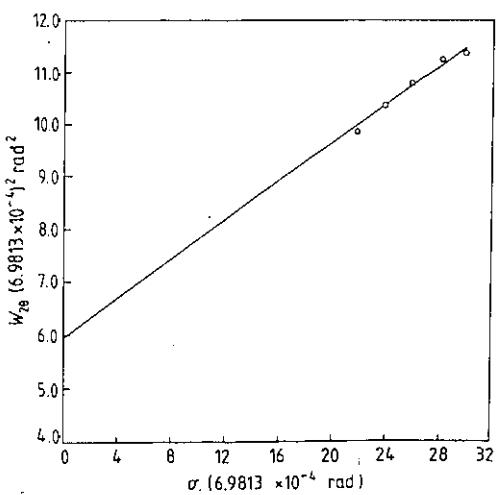

Figure 3. Variance $W_{2\theta}$ against range σ plot for a 342 nm CdSe film deposited at room temperature (303 K).

Table 1. X-ray diffraction lines of CdSe powders. *d* values are calculated and compared with standard *d* values obtained from the powder diffraction file.

Serial No	2θ (deg)	Calculated *d* value (Å)	*hkl*	Standard *d* value (Å)
1	23.80	3.734	100	3.720
2	25.30	3.516	002	3.510
3	27.07	3.290	101	3.290
4	35.02	2.559	102	2.554
5	41.95	2.151	110	2.151
6	45.72	1.982	103	1.980
7	48.08	1.863	200	1.863
8	49.65	1.833	112	1.834
9	50.65	1.800	201	1.800
10	55.80	1.645	202	1.645
11	63.82	1.456	203	1.456
12	66.32	1.407	210	1.407
13	67.73	1.381	211	1.380
14	71.83	1.312	105	1.312
15	76.66	1.241	300	1.241
16	79.34	1.206	213	1.205
17	82.50	1.169	302	1.170
18	86.95	1.120	205	1.120
19	87.31	1.116	106	1.114
20	91.76	1.073	220	1.074
21	96.30	1.032	310	1.032
22	97.20	1.027	222	1.027
23	99.75	1.021	311	1.021
24	101.67	0.994	215	0.993
25	102.06	0.991	312	0.990
26	109.19	0.945	313	0.945

a shift in the peak position of different reflections with respect to the ideal position of a fault-free well annealed sample. Three typical experimental profiles showing the peak shift for hexagonal {002} reflection of CdSe films of different thickness with respect to a well annealed bulk sample are shown in figure 2. The complete diffraction pattern of a film of 280 nm thickness deposited at room temperature and a film of 290 nm thickness deposited at 623 K substrate temperature are shown in figure 1(*b*) and 1(*c*) respectively. Warren and Warekois (1955) have given a relation connecting α with peak shift $\Delta(2\theta)$. The stacking fault probability α is given by

$$\alpha = [2\pi^2/(45\sqrt{3}\tan\theta)]\,\Delta(2\theta^0). \qquad (4)$$

The fault probabilities have been calculated from the shift of the peaks of the x-ray lines of the films with reference to that from a well annealed sample using equation (4). The variance W against range σ plot for a typical CdSe film of 342 nm thickness deposited at room temperature (303 K) is shown in figure 3. The linearity of the plot shows that the background has been adjusted properly.

3. Results and discussion

Figure 1(*a*) shows the x-ray diffraction pattern of CdSe powders. Different peaks are indexed and the values

Table 2. Microstructural parameters for CdSe films of different thickness deposited at room temperature (303 K) in a vacuum.

Film thickness (μm)	Cd/Se (atom %)	Particle size, *P* (nm)	RMS strain $\langle e^2\rangle^{1/2} \times 10^4$	Dislocation density, ρ (10^{14} lines m^{-2})	Stacking fault probability, α
0.280	1.020	37.80	42.53	10.314	0.017
0.342	1.026	48.70	38.84	7.731	0.022
0.503	1.082	60.90	37.67	5.741	0.036
0.673	1.191	81.20	36.86	4.520	0.050
1.007	1.222	91.76	35.68	3.840	0.061
1.410	1.261	94.25	36.62	3.835	0.051
1.725	1.300	94.78	37.88	3.939	0.042

Table 3. Microstructural parameters for CdSe films deposited at different substrate temperatures in a vacuum.

Substrate temperature, T_s (K)	Film thickness (μm)	Cd/Se (atom %)	Particle size, *P* (nm)	RMS strain $\langle e^2\rangle^{1/2} \times 10^4$	Dislocation density, ρ (10^{14} lines m^{-2})	Stacking fault probability, α
373	0.271	1.015	46.4	65.40	13.928	0.050
473	0.340	1.010	54.7	50.20	9.061	0.029
			(27.0)	(34.96)	(23.74)	(0.102)
573	0.310	1.346	86.3	38.82	4.437	0.020
			(30.6)	(28.16)	(18.35)	(0.070)
623	0.290	1.441	94.0	34.12	3.576	0.006
			(37.0)	(19.92)	(10.14)	(0.058)

of interplanar spacing d are calculated and compared with standard d values (*Powder Diffraction File*). The calculated d values and their corresponding indices are given in table 1. The presence of some excess cadmium in the prepared sample is evident from the x-ray diffraction pattern (figure 1(*a*)). The x-ray and electron diffraction patterns show that the films deposited on the glass substrates kept at room temperature have wurtzite structure. It is also observed from the x-ray diffraction patterns that the crystallites in the films deposited at room temperature are preferentially oriented with (002) face parallel to the substrate. The values of the particle size, microstrain, dislocation density and stacking fault probability for the films of different thickness are given in table 2. Corresponding values for the films deposited at different substrate temperatures are compiled in table 3. The variation of crystallite size and RMS strain with thickness of the films is shown in figure 4, and variation of dislocation density and stacking fault probability with thickness is shown in figure 5.

From the x-ray diffraction patterns of CdSe films deposited at different substrate temperatures it has been observed that, as the substrate temperature increases to 473 K and above, the hexagonal (112) peak appears along with the initial hexagonal (002) peak. As the substrate temperature increases the intensity of (002) peak increases and hence also the particle size in this orientation. However, the intensity of the (112) peak belonging to the hexagonal phase which appears at and above 473 K increases with further increases in substrate temperature. In table 3 the particle size, RMS strain, dislocation density and stacking fault probabilities, calculated from the analysis of (112) peaks are given within the addenda below their corresponding values calculated from (002) peaks. The variations of different microstructural parameters with substrate temperature T_s are depicted in figures 6 and 7.

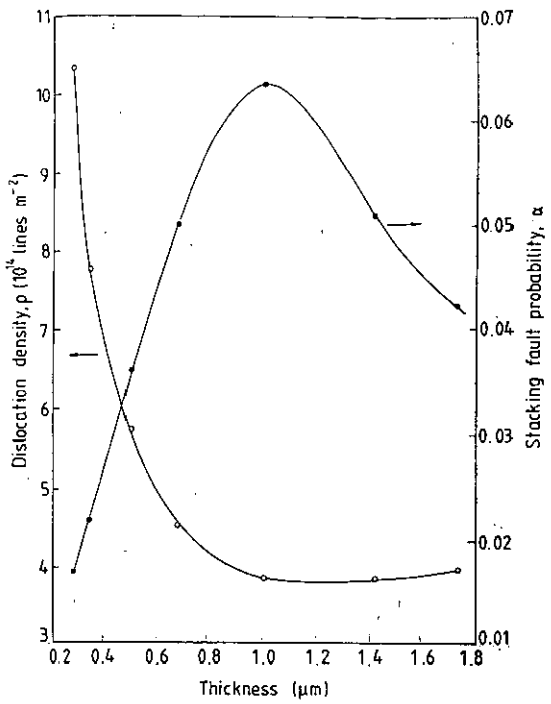

Figure 5. (*a*) Dislocation density and (*b*) stacking fault probability against film thickness for the CdSe films deposited at room temperature (303 K).

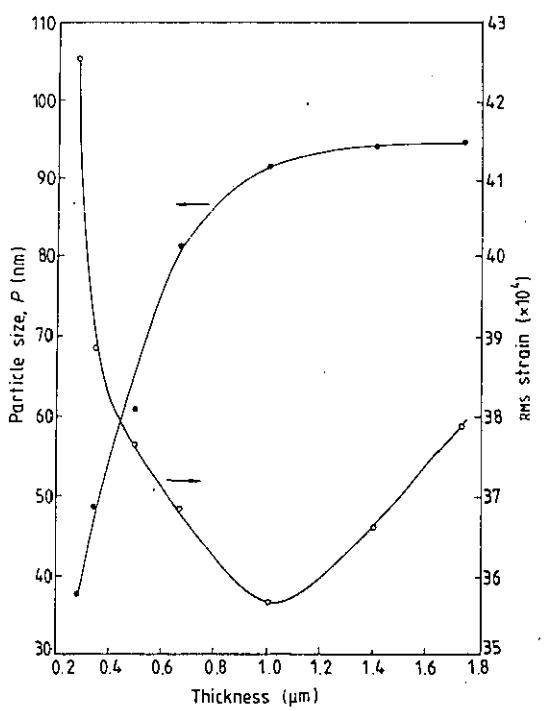

Figure 4. (*a*) Particle size and (*b*) microstrain against film thickness for the CdSe films deposited at room temperature (303 K).

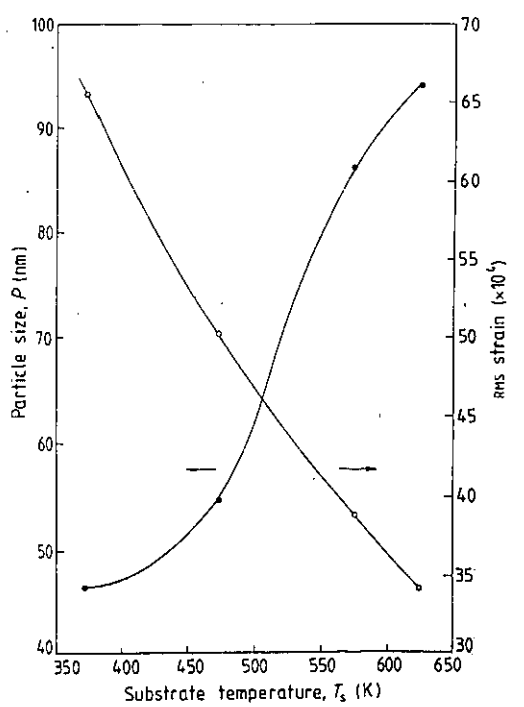

Figure 6. (*a*) Particle size and (*b*) microstrain against substrate temperature of CdSe films (~300 nm).

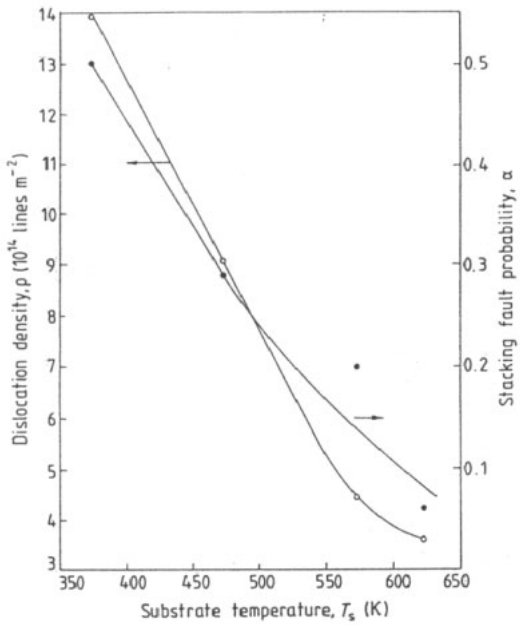

Figure 7. (*a*) Dislocation density and (*b*) stacking fault probability against substrate temperature of CdSe films (~300 nm).

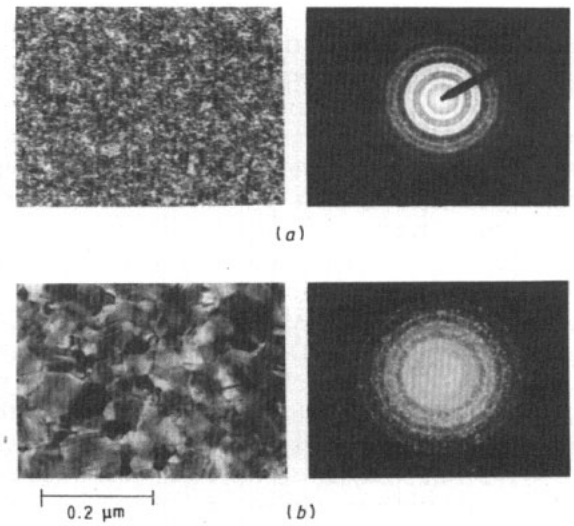

Figure 8. TEM and TED photographs for CdSe films deposited at (*a*) room temperature (303 K) and (*b*) 623 K.

It has been observed that the crystallite size value steeply increases with the film thickness up to 1.0 μm and then increases gradually. The microstrain value decreases up to 1.0 μm and then increases with the thickness of the films. The dislocation density decreases up to this thickness and stacking fault probability becomes maximum. At this thickness, microstrain attains its minimum value. The release in RMS strain takes place with the formation of stacking faults and hence causes an increase in the stacking fault probability value. Above this thickness, although the particle size value increases gradually due to increase of RMS strain, the dislocation density slowly increases.

A sharp increase of particle size and decrease of RMS strain value with increases in substrate temperature are very clear from figure 6. Figure 7 shows that both the dislocation density and stacking fault probability decrease with increasing substrate temperature. In figure 8 the transmission electron micrographs and transmission electron diffraction patterns of the CdSe films deposited at room temperature (303 K) and at 623 K are shown. Increase of particle size with increase of substrate temperature from room temperature to 623 K is quite high, as observed from electron micrographs in comparison with the results obtained from line profile analysis. The increase of particle size with the increase of substrate temperature is also clear from the electron diffraction patterns, where the 'spotty' nature of the diffraction rings increases with increasing substrate temperature. Such an increase of particle size with substrate temperature has also been reported by Shallcross (1963), Naguib *et al* (1979), Chase *et al* (1980) and Hyugaji and Miura (1985). According to Naguib *et al* (1979) the average grain size evaluated from the TEM observation increased from 5 to 40 nm as the substrate temperature increased from room temperature to 473 K, where the deposition rate and thickness were 60 nm min^{-1} and 50 nm respectively. Also, when the film thickness was about one micrometre, the average grain size was evaluated as 80 nm by x-ray diffraction. According to the TEM observation of Chase *et al* (1980) for CdSe films deposited on Corning 7059 glass substrates at 353–373 K substrate temperature, the grain size was 5–20 nm in diameter. Hyugaji and Miura (1985) obtained particle sizes about ten times larger (TEM observation) for CdSe films deposited on glass substrates by molecular beam deposition (MBD). The rate of deposition was about 6 nm min^{-1} and the substrate temperature varied from room temperature to 573 K. However, in the present study, although the evaluated particle size values (line profile analysis) are not as high as reported by Hyugaji and Miura (1985), they are higher than the reported values of other workers. The success of the present work lies not in particle size, but in its deposition rate. We have obtained high values of particle size with 120 nm min^{-1} deposition rate. The tabulated values of particle size are somewhat less than the particle sizes observed from the TEM photographs.

With increases in film thickness, selenium vacancies in the films increase. The n-type conductivity of the films is normally attributed to such selenium vacancies. However, with the increase of substrate temperature up to 473 K, the stoichiometry of the films improves and it further degrades with further increases of substrate temperature. A similar observation has been made by Hyugaji and Miura (1985). Deviation of stoichiometry beyond 473 K is due to the re-evaporation of Se from the surface of the growing film. Although up to 473 K substrate temperature the stoichiometry improved, the particle size increased significantly up to 623 K. Therefore we can conclude that the increase of particle size with the increase of substrate temperature

is not due to its change in stoichiometry, it is due to the increase in mobility of the evaporated atoms at the substrate. Similar improvements of stoichiometry up to 430 K substrate temperature have been observed by Raoult *et al* (1989). From their resistivity measurements these workers also observed that the stoichiometry degrades further due to further increases in substrate temperature.

Although II–VI compounds can crystallize in cubic zinc blende structure as well as in hexagonal wurtzite structure and many workers (Shalimova *et al* 1970, Nagata and Agata 1951, Dolega 1963) have reported the formation of different phases in CdSe, we have not observed any phase transformation in our CdSe thin films by varying their thickness or substrate temperature. This result is similar to the observation made by Boichot and Wilman (1980) in their CdSe films deposited at room temperature. By preparing CdSe films in a quasi-closed system, Shalimova *et al* (1970) observed the hexagonal phase to be favourable for cadmium excess, whereas Nagata and Agata (1951) reported the formation of cubic CdSe at the cadmium interface and hexagonal CdSe at the selenium interface for their selenium rectifiers covered with cadmium. The same interpretation follows from the results of Dolega (1963) who prepared CdSe films by co-evaporating cadmium and selenium onto glass substrates followed by an annealing treatment. The films were found to contain the cubic phase almost exclusively, with a cadmium excess. A mixture of cubic and hexagonal phases in CdSe films deposited on glass substrates at different substrate temperatures is observed by Moore *et al* (1975). According to their observation, the proportion of hexagonal phase increases with increase in substrate temperature but there is always a significant amount of the cubic phase. No pure hexagonal or cubic phase is observed by them even for films deposited at 673 K or produced by excess selenium flux. However, this anomaly can be explained by the argument given by Daweritz (1974). According to him the incorporation of the atoms in a non-stoichiometric ratio causes a deformation of the coordination polyhedron, which can be related to variation of the intensity and direction of polarization forces (Spinulescu-Carnaru 1966). The cubic symmetry of an ideal tetrahedron is lost due to elongation or shortening of inter-atomic distance, and as a result hexagonal symmetry occurs.

In the case of our CdSe films, formation of the hexagonal phase is perhaps due to the non-stoichiometric ratio of Cd and Se in the films. The excess of either component (Cd in the present case) has caused the deviation of the c_0/a_0 value from the ideal 1.633 value due to a deviation of u (bond length 0.375) and increased the probability of appearance of hexagonal phase.

4. Conclusions

The microstructural parameters of the CdSe films deposited on glass substrates are critically dependent on the thickness and the substrate temperature of the films. Crystallite size and stacking fault probability increase sharply up to 1.0 μm thickness of the films, beyond which crystallite size increases gradually but stacking fault probability decreases. At this thickness (1.0 μm), RMS strain attains its minimum value causing an increase in stacking fault probability, whereas the fault-like dislocation density decreases with increasing film thickness. With the increase of substrate temperature up to 623 K, crystallite size of the films increases and RMS strain, dislocation density and stacking fault probability decrease. The crystallite size value depends more critically on the thickness and substrate temperature than on the stoichiometry of the film material.

References

Boudrau R A and Rauh R D 1982 *Sol. Energy Mat.* **7** 385
Boichot S J and Wilman H 1980 *J. Phys. D: Appl. Phys.* **13** 45
Curran J S, Naguyen Du, Phillippe R and Stremsdoerfer G 1986 *Thin Solid Films* **144** 117
Chase B D, Collins G C S and Huntley F A 1980 *Thin Solid Films* **67** 207
Dolega U 1963 *Z. Naturforsch.* **18**a 809
Daweritz L 1974 *J. Cryst. Growth* **23** 307
El-Shazly A A, El-Nady L M, El-Nahass M M, El-Shair H T and Morsy A Y 1986 *Opt. Pura Appl.* **19** 23
Givargizov E I 1974 *Sov. Phys. Dokl.* **18** 458
Heller A, Chang K G and Miller B 1977 *J. Electrochem Soc.* **124** 697
Hirsch P B 1956 *Prog. Math. Phys.* **6** 236
Hyugaji M and Miura T 1985 *Japan. J. Appl. Phys.* **24** 950
Miller D J and Hanemann D 1981 *Sol. Energy Mat.* **4** 223
Mitra G B 1964 *Acta Crystallogr.* **17** 765
Mitra G B and Misra N K 1966 *Br. J. Appl. Phys.* **17** 1319
Moore R M, Fischer J T and Kozielec F Jr 1975 *Thin Solid Films* **26** 363
Naguib H M, Nentwich H and Westwood W D 1979 *J. Vac. Sci. Technol.* **16** 217
Nagata S and Agata K 1951 *J. Phys. Soc. Japan* **6** 523
Powder Diffraction File vol PDIS-10iRB set 8 card 495
Ratcheva-Stambolieva T M, Tchistyakov Yu D, Krasulin G A, Vanyukov A V and Djoglev H D 1973 *Phys. Status Solidi* a **16** 315
Raoult F, Fortin B and Colin Y 1989 *Thin Solid Films* **182** 1
Samarath N, Luo H, Furdyna J K, Qadri S B, Lee Y R, Ramdas A K and Otsuka N 1990 *J. Electron. Mat.* **19** 543
Santhanam S, Samantaray B K and Chaudhuri A K 1982 *J. Phys. D: Appl. Phys.* **15** 2531
Shalimova K V, Rogge K and Botnev A F 1970 *Kristallogr.* **15** 342
Shallcross F V 1963 *RCA Rev.* **24** 676
Spinulescu-Carnaru I 1966 *Phys. Status Solidi* **18** 769
Thutupalli G M K and Tomlin S G 1976 *J. Phys. D: Appl. Phys.* **9** 1639
Ueno Y, Kaigawa H, Ohasi T, Suigiura T and Minoura H 1987 *Sol. Energy Mat.* **5** 421
Warren B E and Warekois E P 1955 *Acta Metall.* **3** 473
Williamson G B and Smallman R C 1956 *Phil. Mag.* **1** 34
Yim W M and Stofko E J 1974 *J. Electrochem. Soc.* **121** 965